

Supplementary Information

Electrochemical chiral recognition of tryptophan enantiomers by using chiral polyaniline and β -CD-MOF

Jiamin Liang^[1], Yuxin Song^[1], Huan Xing^[1], Liang Ma^[1], Fengxia Wang^[1], Mingfang Zhang^[1], Hongli Zhang^{[2]*}, Gang Zou^{[2]*} and Guang Yang^{[1]*}

^[1]*Department of Chemistry and Chemical engineering, College of Chemistry, Chemical Engineering and Resource Utilization, Northeast Forestry University, Hexing Road 26, Harbin 150040, P. R. China.*

^[2]*Key Laboratory of Precision and Intelligent Chemistry, School of Chemistry and Materials Science, University of Science and Technology of China, Hefei, Anhui, China.*

*Corresponding Author:

Guang Yang, E-mail: guangyang@nefu.edu.cn; gangzou@ustc.edu.cn; zh11992@ustc.edu.cn

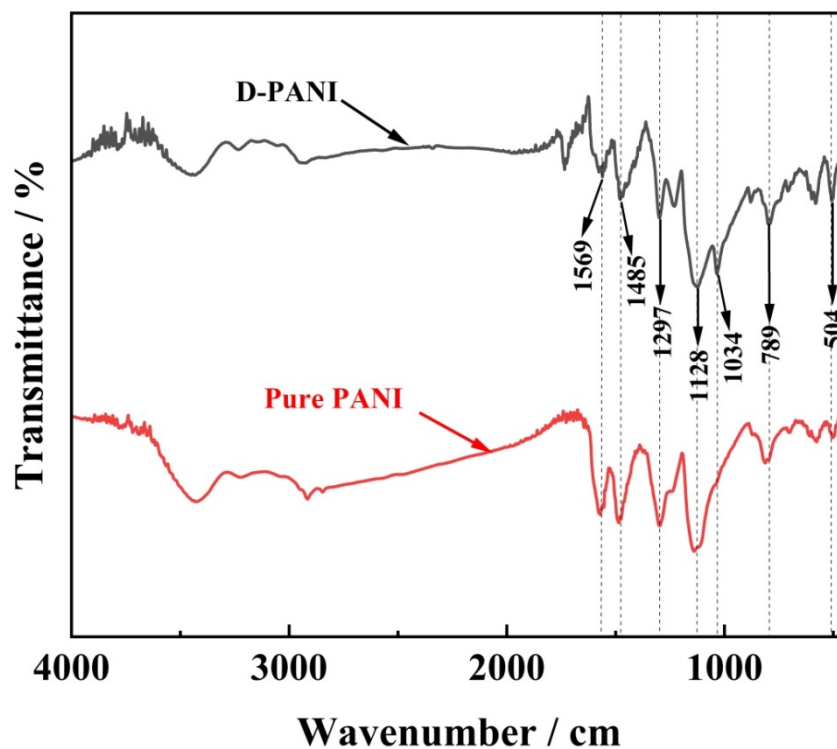


Fig. S1 The FT-IR spectra of D-PANI (black line) and pure PANI (red line).

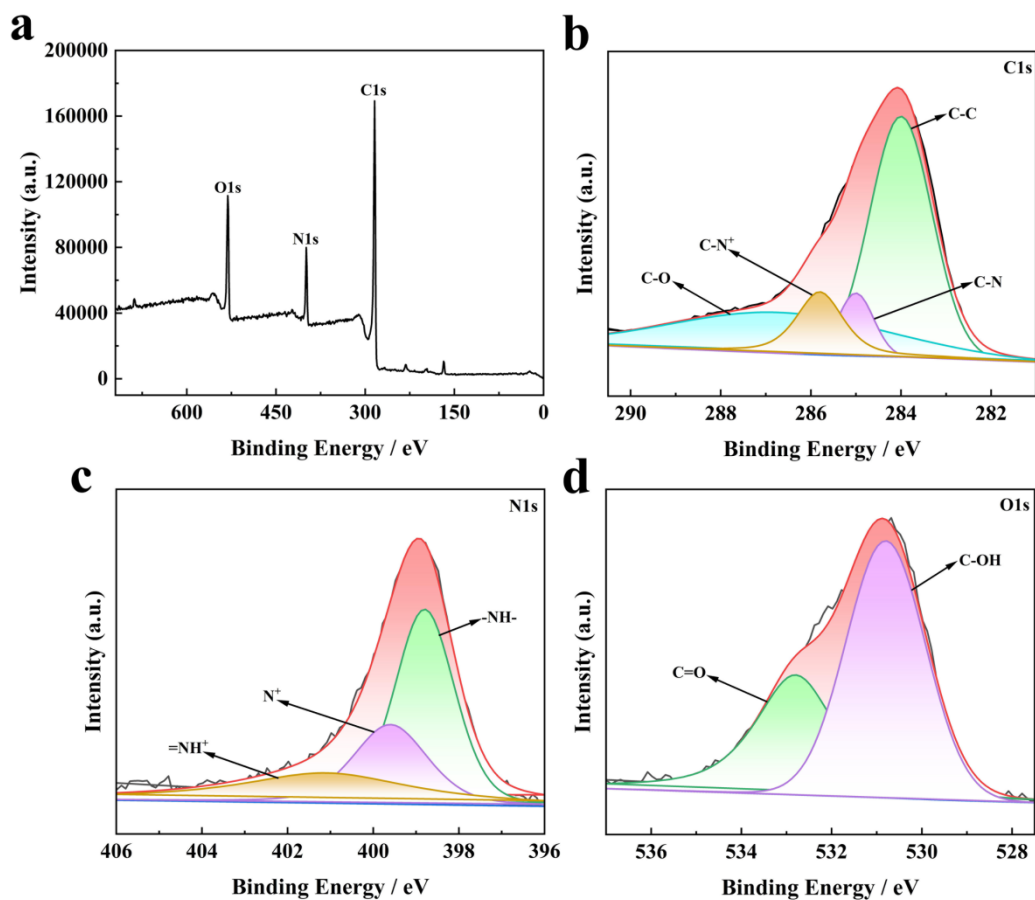


Fig. S2 (a) The wide survey XPS spectra (b) C1s (c) N1s and (d) O1s of PANI.

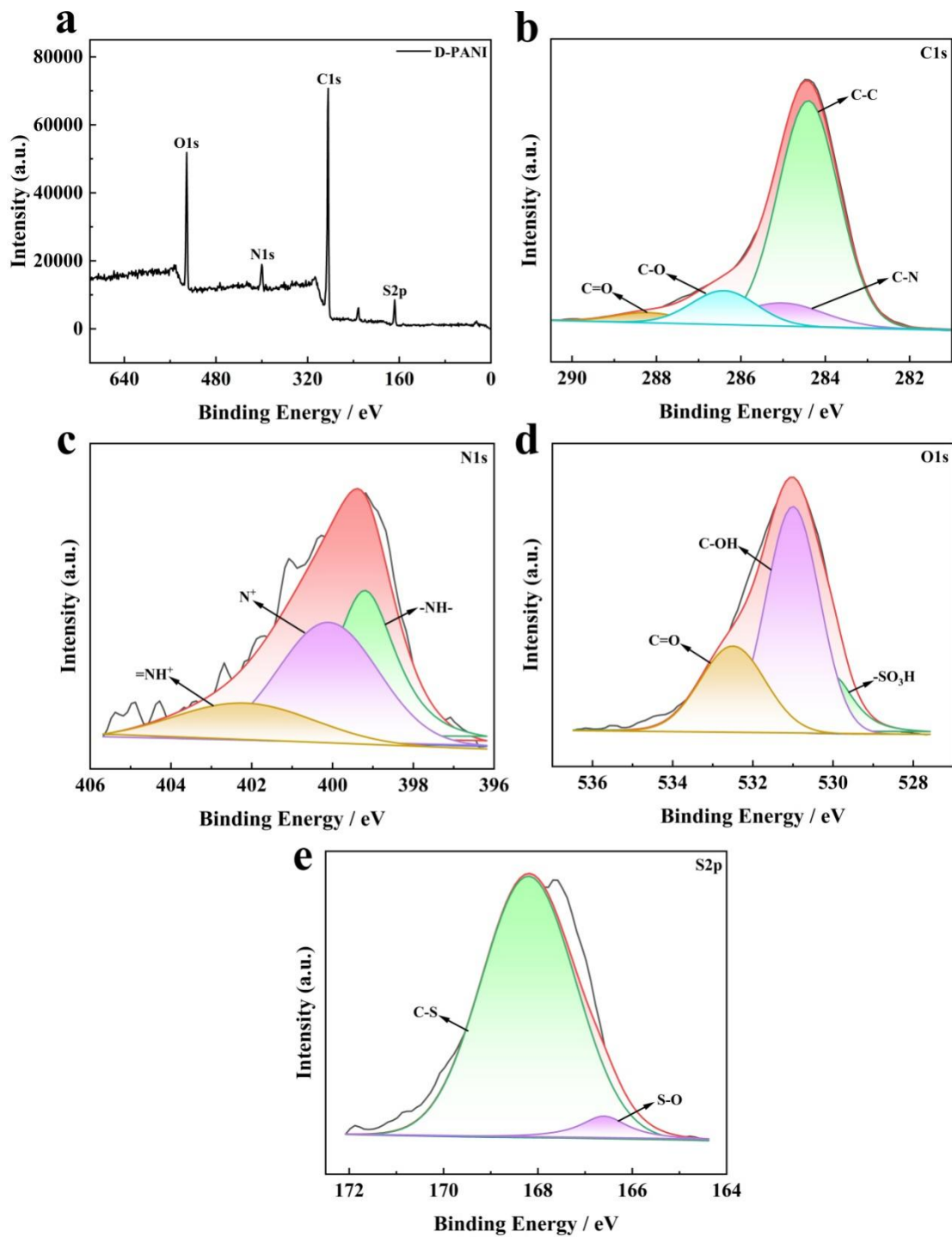


Fig. S3 (a) The wide survey XPS spectra (b) C1s (c) N1s (d) O1s and (e) S2p of D-PANI.

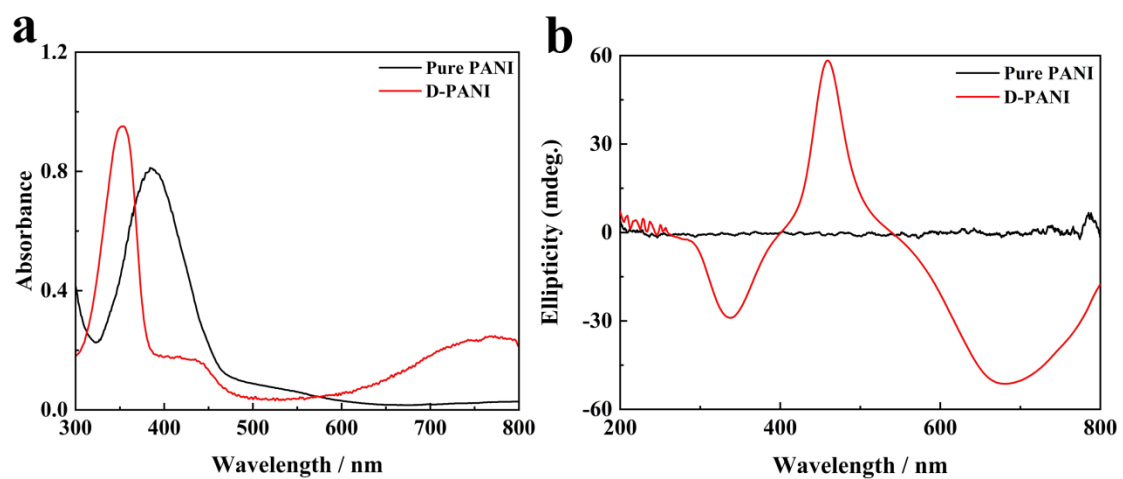


Fig. S4 (a) The UV-vis spectra and (b) CD spectra of pure PANI (black line) and D-PANI (red line).

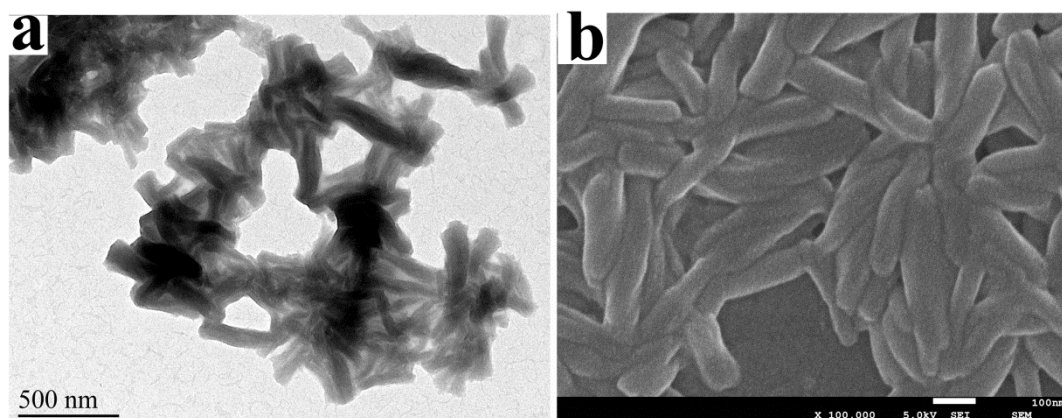


Fig. S5 The (a) TEM and (b) SEM image of D-PANI.

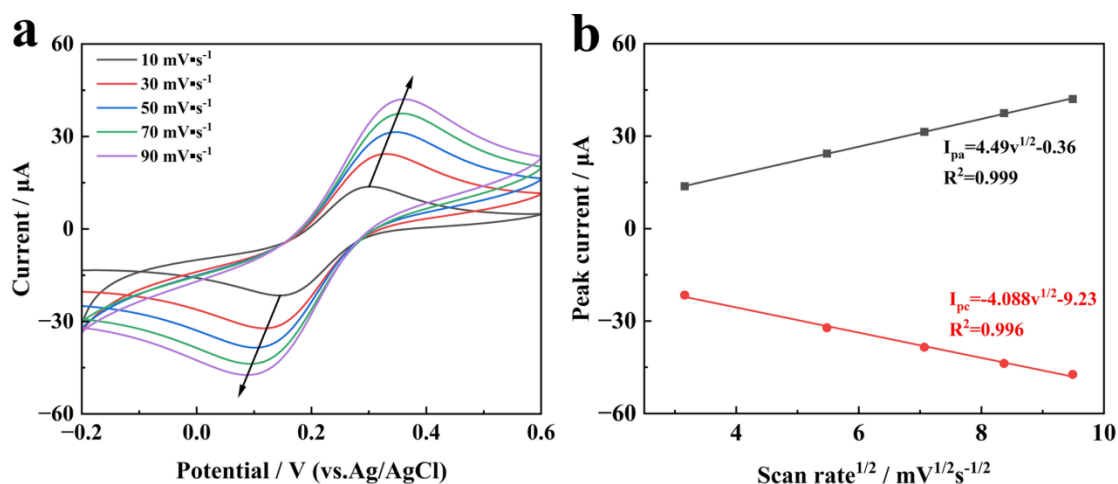


Fig. S6 (a) The CVs of bare GCE in 1 mM $[\text{Fe}(\text{CN})_6]^{3-/4-}$ containing 0.1 M KCl at increasing scan rates: 10, 30, 50, 70 and 90 mV s^{-1} . (b) The peak currents as a function of scan rate for the determination of the effective working surface area.

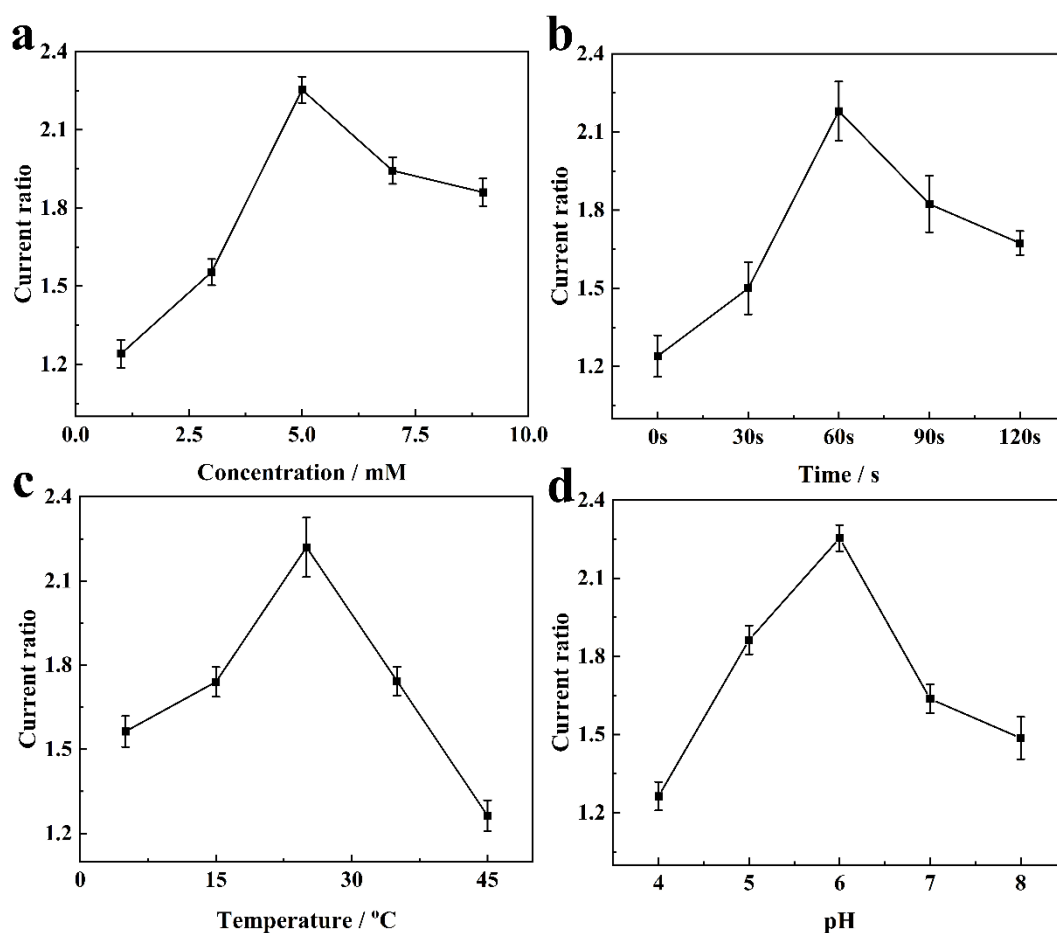


Fig. S7 Influence of (a) concentration of Trp isomers, (b) incubation time, (c) temperature and (d) solution pH value on the DPV response of the GCE/ β -CD-MOF/D-PANI towards Trp isomers detection.

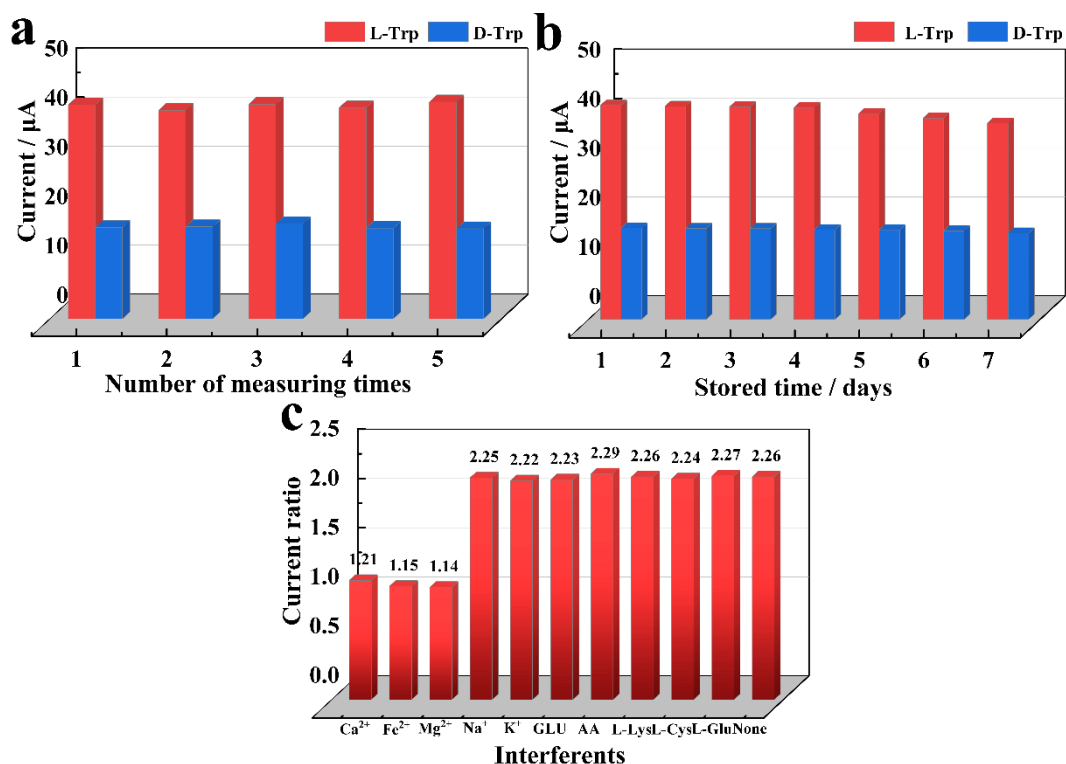


Fig. S8 The reproducibility, stability and anti-interference ability of the GCE/ β -CD-MOF/D-PANI: (a) The current of five independent DPV measurements for the discrimination of Trp enantiomers; (b) The current of modified electrode was stored in a refrigerator for seven days; (c) The current ratio (I_L/I_D) of GCE/ β -CD-MOF/D-PANI without and with the interfering material of 5 mM (Ca^{2+} , Fe^{2+} , Mg^{2+} , Na^+ , K^+ , glucose (GLU), ascorbic acid (AA), L-lysine (L-Lys), L-cysteine (L-Cys), and L-glutamic (L-Glu)).

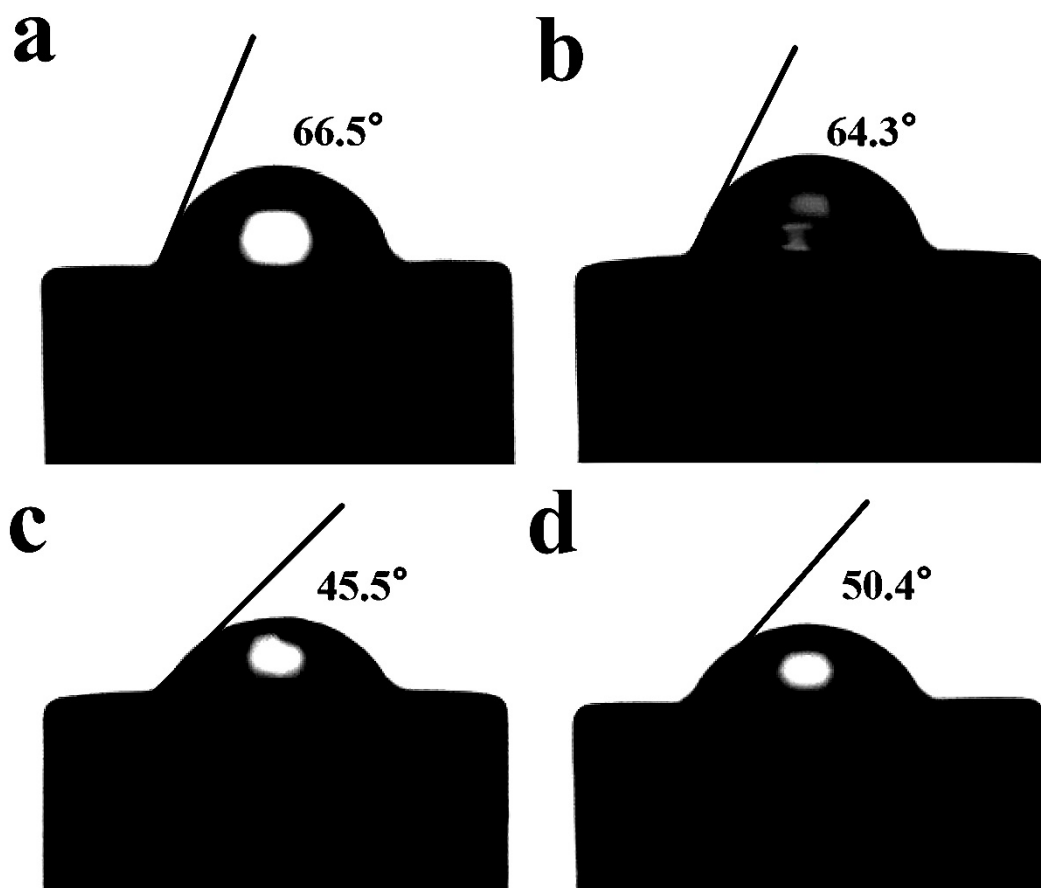


Fig. S9 The photographs of water droplet shape of different electrodes: (a) bare GCE, (b) GCE/ β -CD-MOF/D-PANI, (c) GCE/ β -CD-MOF/D-PANI dipped in L-Trp solution and (d) GCE/ β -CD-MOF/D-PANI dipped in D-Trp solution.

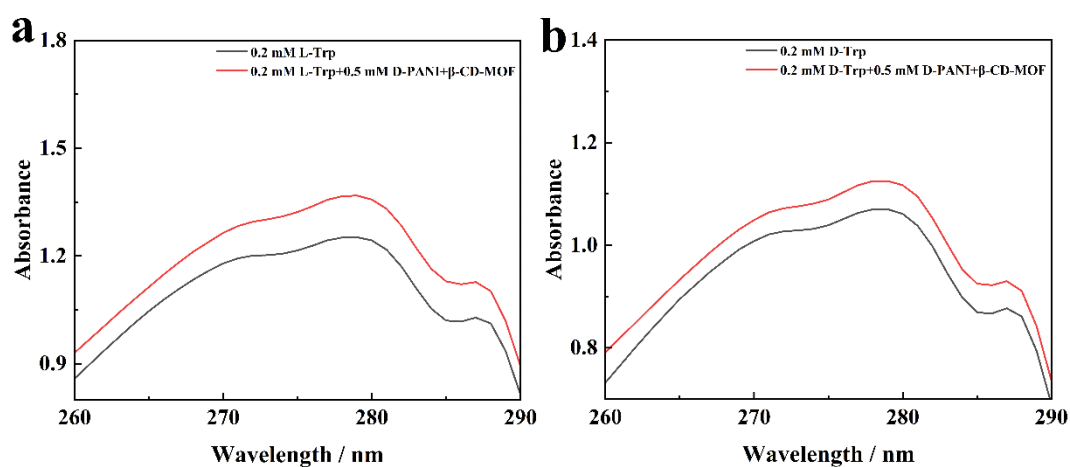


Fig. S10 UV-vis spectra of (a) L-Trp and (b) D-Trp before and after incorporation with β -CD-MOF+D-PANI (0.5 mM).

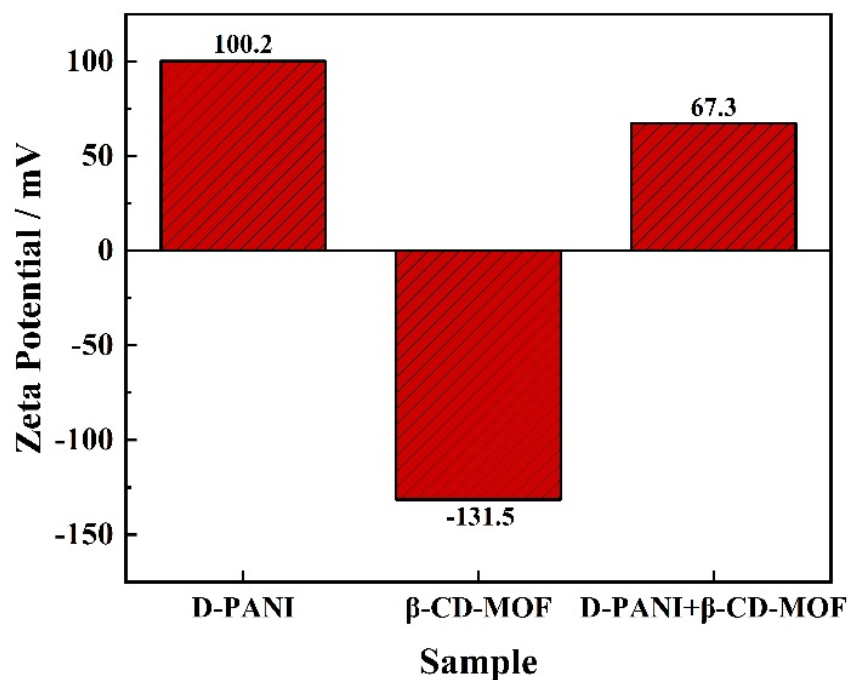


Fig. S11 The zeta potential values for D-PANI, β -CD-MOF and D-PANI+ β -CD-MOF.

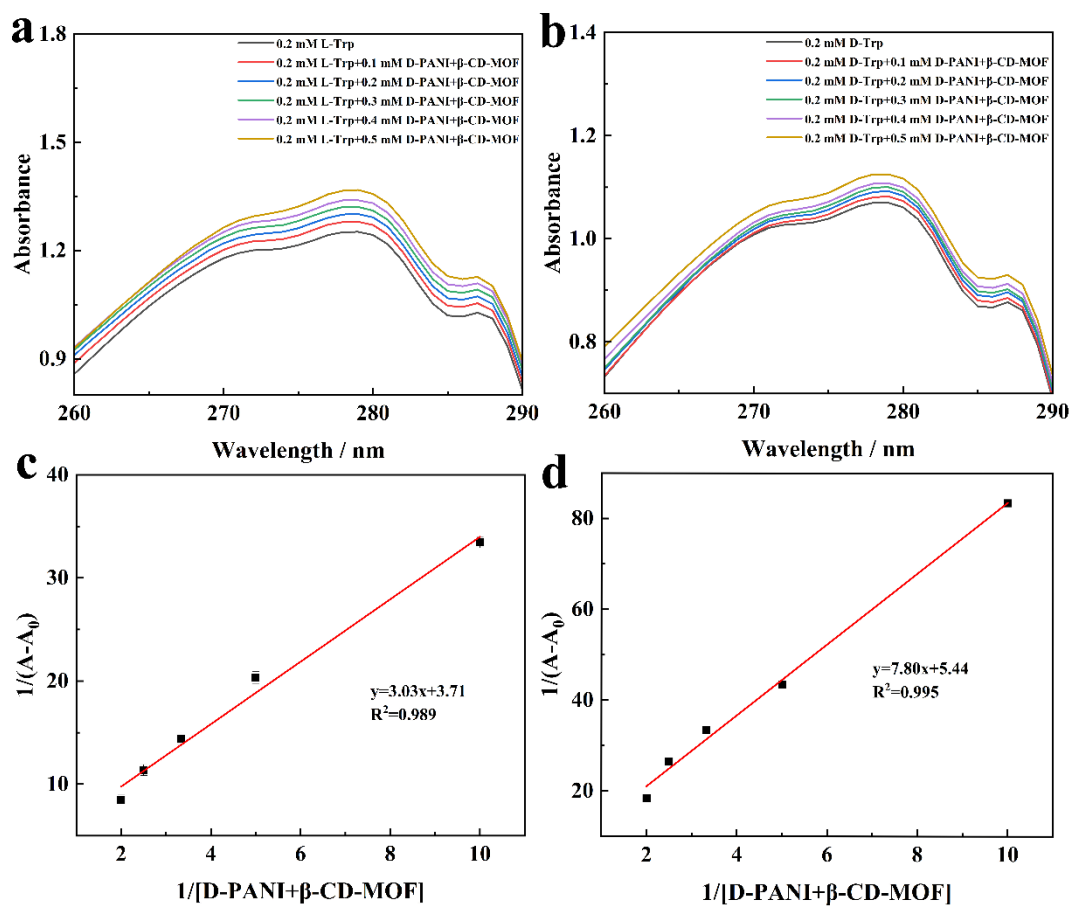


Fig. S12 The UV spectra of 0.2 mM L-Trp (a) and D-Trp (b) after addition of β -CD-MOF+D-PANI of various concentrations. Double reciprocal plots of L-Trp (c) and D-Trp (d) contained β -CD-MOF+D-PANI.

Table S1 Detection of L-Trp in actual samples (n=6)

Sample	CL ^a (μM)	Added (μM)	Founded (μM)	RSD (%)	Recovery (%)
Human urine	2.2	0.5	2.79±0.103	3.7	103.3
		1.0	3.13±0.135	4.3	97.8
		10.0	12.28±0.381	3.1	100.6
		50.0	53.18±2.180	4.1	101.9

^a L-Trp content in real samples.

Table S2 Detection of D-Trp in actual samples (n = 6)

Sample	CD ^b (μM)	Added (μM)	Founded (μM)	RSD (%)	Recovery (%)
Human urine	3.1	0.5	3.69±0.166	4.5	102.5
		1.0	4.25±0.135	3.3	103.7
		10.0	12.73±0.535	4.2	97.2
		50.0	52.73±1.951	3.7	99.3

^b D-Trp content in real samples.